Article:
Zhu, H, Li, XK, Han, F et al. (5 more authors) (2016) The effect of pitch-based carbon fiber microstructure and composition on the formation and growth of SiC whiskers via reaction of such fibers with silicon sources. Carbon, 99. pp. 174-185. ISSN 0008-6223

https://doi.org/10.1016/j.carbon.2015.12.002

The effect of pitch-based carbon fiber microstructure and composition on the formation and growth of SiC whiskers via reaction of such fibers with silicon sources

Hui Zhu[a,b], Xuanke Li[a,b *] Fei Han[b], Zhijun Dong[a], Guanming Yuan[a], Guozhi Ma[b], Aidan Westwood[c]， Kejie He[d]

[a] The State Key Laboratory of Refractories and Metallurgy, Wuhan University of Science and Technology, Wuhan, Hubei 430081, P. R. China

[b] The research center for advanced carbon materials, Hunan University, Changsha, Hunan 410082, P. R. China

[c] Institute for Materials Research, School of Chemical and Process Engineering, University of Leeds, Leeds, LS2 9JT, U.K.

[d] Advanced research center, Central South University, Changsha,Hunan 410083, P. R. China.

ABSTRACT

The formation and growth of silicon carbide whiskers (SiCw) have been investigated by reaction of silicon sources at 1400 ºC with pitch-based carbon fibers possessing various microstructures. Isotropic and anisotropic pitch-based carbon fibers treated at various temperatures were employed as carbon sources. Silicon sources include

* Corresponding author: Fax: +86 27 86556906.
E-mail address: xkli8524@sina.com (X. Li).

silicon powder and a mixture of silicon and silica powder. The reaction of 1000 ºC heat-treated carbon fibers containing a certain content of oxygen with silicon powders is also reported. A reasonable yield of monocrystalline and polycrystalline SiC whiskers can be achieved by the reaction of the isotropic and anisotropic pitch-based carbon fibers treated at 1000 and 2000 ºC with the mixture of silicon and silica. The critical factors for promoting the formation of SiC whiskers are that the carbon sources should possess turbostratically stacked graphite structure and appropriate grain size. The presence of SiO, which originated from the reaction of silicon with silica or with water vapor derived from pyrolysis of carbon fibers, is another necessary condition for formation of SiCw during these reaction processes.

1. Introduction

SiC whiskers (SiCw) have attracted considerable attention due to their excellent mechanical, electrical and optical properties, and they are extensively used for reinforcing advanced composites with various matrices and in electronic devices, operating under extremely harsh conditions [1-10]. Due to the great interest in silicon carbide whiskers for materials technology, numerous methods have been developed to prepare SiC whiskers, including pyrolysis of polyureasilazane precursor [11], carbon nanotube-confined reaction [12], chemical vapor deposition [13], sol-gel synthesis [14,15], carbothermal reduction [16,17], and direct chemical reactions [18]. However, existing syntheses for the large-scale production of SiC whiskers generally yield low purity products with various structural defects [8,19] or require costly precursors [11],

rigorous handing of volatile reagents [13] and high temperature [18].

In our work on the synthesis of SiC coating on carbon fibers with various microstructures by reacting the fibers with silicon powders, the formation of SiCw was observed on some kinds of carbon fibers, but interestingly, SiCw could not be seen on the surface of others. In addition, the yield of SiCw varied with the type of carbon fiber. This suggests that the nucleation and growth of SiCw may have a close relation with the structure of the carbon source and nature of the silicon source. Coincidentally, Satapathy et al. [20] also reported the casual formation of SiC nanorods by the reaction of silicon powder with amorphous carbon below 1400 °C, but no likely interpretation was given.

Kholmanov et al. [21] reported a similar phenomenon whereby the presence of a trace of oxygen derived from reagents or shielding gas facilitated the formation of SiO gas, thus leading to the formation of SiC whiskers by a vapor-solid (VS) mechanism. Nevertheless, the influence of silicon source on the formation of SiCw by the VS mechanism is still under study and remains to be confirmed unequivocally.

At the same time, the influence of the carbon source on the nucleation and growth of SiCw by reaction of SiO with C also attracts particular attention. Indeed, Zhou et al. [22] was first to propose that the reactivity and atomic configuration of carbon nanotubes were crucial factors governing the formation of SiCw by heating a mixture of carbon nanotubes and silicon monoxide. In a subsequent study, SiC whiskers were synthesized successfully by reacting activated carbon fibers, carbon nanotubes, carbon fibers and graphite with gaseous SiO at 1200-1300, 1400 , 1500 and 1600 ºC,

respectively [12,19,23,24]. Thus, SiC whiskers with various yields and morphologies were synthesized at various temperatures on different carbon sources, indicating that the carbon sources have a significant influence on the formation and growth of SiCw. The mechanism was considered to be epitaxial growth of SiCw on some random spots of carbon sources [23]. However, the influence of the carbon source on the formation of SiCw is still unclear. Therefore, the formation and growth mechanism of SiC whiskers as it relates to the silicon source species and the structure of the carbon source, still needs to be elucidated in order to underpin technology for the large-scale preparation of SiC whiskers.

In this work, highly oriented carbon fibers and general purpose carbon fibers derived from an anisotropic mesophase pitch and an isotropic coal tar pitch, respectively, and treated at various temperatures were used as carbon sources for the preparation of SiC whiskers. The reactions of these carbon fibers with silicon powder or a mixture of silicon and silica powders were investigated to explore the influence of gaseous SiO on the formation and growth of SiCw. The objective of this work is hence to clarify the possible nucleation and growth mechanisms of SiCw and how these correlate with the carbon sources' microstructure and the type of silicon source.

2. Experimental

2.1 The preparation of pitch-based carbon fibers

Commercial isotropic pitch and naphthalene-derived synthetic mesophase pitch purchased from Jining Carbon and Mitsubishi Gas Chemical Corporation, were used

as raw materials for melt-spinning of round-shaped isotropic and anisotropic pitch fibers, respectively. The two kinds of as-spun pitch fibers were stabilized at 240-250 ºC for 10-20 h in a flowing oxygen atmosphere, carbonized at 450 ºC for 1 h and subsequently carbonized at 1000 ºC for 1 h under nitrogen atmosphere in a tube furnace using a heating rate of 1 ºC/min. The carbonized fibers were finally heat-treated under flowing argon atmosphere at 2000 or 3000 ºC for 15 min with a heating rate of 15 ºC/min. These isotropic carbon fibers (IF) and anisotropic pitch-based carbon fibers (AF), heat-treated at 1000, 2000 and 3000 °C were used as carbon sources, labelled as IF1000, IF2000, IF3000, AF1000, AF2000 and AF3000, respectively.

2.2 The preparation of SiC whiskers

Silicon and silica powders (ca. 300 mesh and purity of 99.9%), purchased from Beijing New Material Technical Co. Ltd. in China, were used as silicon sources. Syntheses of SiC whiskers were carried out by reacting the carbon fibers with silicon at a molar ratio of C:Si = 1:1, or with a mixture of silicon and silica powders at a molar ratio of C:Si:SiO_2 = 2:1:1 at the required temperature under flowing argon atmosphere.

The silicon source was placed in a covered graphite crucible and covered by carbon fibers of length 2 cm in alternating layers to guarantee more homogeneous reaction. The covered graphite crucible was placed in a vertical graphitizing furnace and vacuum purged before argon gas was introduced to a pressure of 0.1 MPa and this process was the repeated. The crucible was then heated to the required temperature for

1 h under a flowing argon atmosphere.

2.3 Characterization of raw materials and as-prepared samples

The phases present in the carbon fibers were identified by X-ray diffraction (XRD) using a Philips X'Pert Pro MPD instrument with Cu K_α radiation. The working voltage and current for the Cu target were 40 kV and 40 mA, respectively. Crystalline parameters of graphite crystals were approximately calculated based on the Scherrer equation

$$L=K\lambda/\beta\cos\theta$$

The diffraction angles of {002} and {100} planes were carefully corrected by the use of silicon powder as an internal reference. Operation and data processing followed the standard procedure for X-ray diffraction measurements on carbon materials [25]. The carbon, oxygen and hydrogen contents of carbon fibers were analyzed by a Vario EL Ⅲ elemental analyzer made by ELEMENTAR, Germany. The surface morphology and microstructure of the carbon fibers and SiCw were investigated using a NOVA400 NANOSEM field emission scanning electron microscope (FESEM) and a Titan G2 60-300 image corrector / field emission gun transmission electron microscope (FEGTEM) with Super-X energy dispersive X-ray spectroscopy attachment. In order to link information on product microstructure and elemental composition and content, atomic lattice resolution transmission electron microscopy (HRTEM), selected-area electron diffraction (SAED) analyses and energy dispersive X-ray spectroscopy (EDS) were conducted on representative areas/fibres. Statistical analysis of the range of SiC whisker diameters was also carried out by measuring

about 150 whiskers in the TEM. Detailed analyses of gases were performed in a Netzsch STA 449C TG-DTA thermoanalyzer coupled with a Balzers Thermostar Quadrupole Mass Spectrometer (MS). Approximately 15 mg of sample was heated from room temperature to 1000 ºC at a linear heating rate of 10 ºC/min under argon with a flow rate of 30 mL/min. The MS signals were processed by smoothing, baseline subtraction, and then normalized to the mass of the sample and the maximum of the total intensity of the experiment. Special attention was paid to the evolution of H_2O.

3. Results and discussion

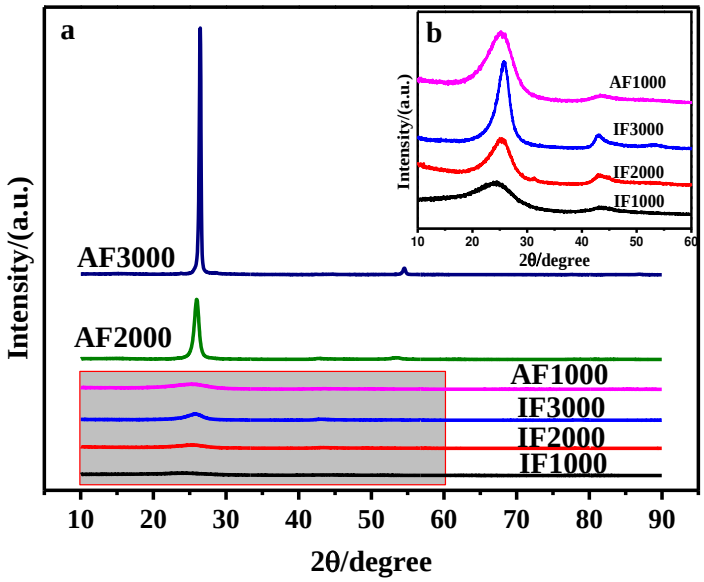

Fig. 1 XRD patterns of the (a) isotropic and anisotropic pitch-based carbon fibers heat-treated at various temperatures and (b) magnified XRD pattern of the shaded area in Fig. 1(a).

Fig. 1 illustrates the XRD patterns of the isotropic and anisotropic pitch-based carbon fibers heat-treated at various temperatures. In comparison with AF2000 and AF3000, the {002} plane diffraction peaks (shown in Fig. 1(a)) of isotropic carbon fibers treated at various temperatures and AF1000 are very weak. Fig. 1(b) shows the magnified patterns of IF1000, IF2000, IF3000 and AF1000. A broad peak at around 2θ=25.5°, corresponding to the {002} reflections of the graphite structure [26], can be observed. With the increase of heat-treatment temperature, the intensity of {002} diffraction peaks of carbon fibers increases and the {002} plane diffraction peaks gradually shift to higher angle and show increased symmetry. Sharpening of the peaks indicates that the crystal size in the carbon fibers increases with the heat-treatment temperature. The increase in intensity of the {002} planes' diffraction peak for anisotropic carbon fibers (shown in Fig. 1(a)) is much higher than that for isotropic carbon fibers with increasing heat-treatment temperature, indicating the graphitizing and non-graphitizing characters of anisotropic and isotropic carbon fibers, respectively. It also suggests the rapid growth of microcrystals and apparent enhancement of ordering in the internal structure of the anisotropic graphite fibers. In the XRD pattern of AF3000, only peaks at 2θ = 26.5 and 54.3° corresponding to the {002} and {004} planes of graphite can be observed, which suggests that these anisotropic graphitized fibers are highly oriented. On the other hand, the XRD pattern of IF3000 shows two broad and weak peaks at around 2θ = 25.5 and 43° corresponding to the {002} and {100} planes of turbostratic graphite, respectively, revealing the disordered structural character of the isotropic carbon fibers.

Crystalline parameters, calculated from XRD results, are listed in Table 1. These parameters quantitatively illustrate the differences in microstructure between the carbon fibers. The decrease of d_{002} and the increase of the $La_{(100)}$, $Lc_{(002)}$ and d_{100}

Table 1 Crystalline parameters of carbon fibers heat-treated at different temperatures

Sample	d_{002}/nm	$Lc_{(002)}$/nm	d_{100}	$La_{(100)}$ /nm
IF1000	0.3668	1.2	0.2078	4.5
IF2000	0.3514	1.7	0.2092	5.8
IF3000	0.3467	3.3	0.2106	8.0
AF1000	0.3529	1.4	0.2079	5.1
AF2000	0.3422	13.6	0.2115	13.4
AF3000	0.3368	39.7	0.2130	78.9

values are clearly apparent for both types of carbon fiber with increasing heat-treatment temperature. This indicates that higher heat-treatment temperature is more beneficial to the ordering and growth of graphite crystals. In comparison with isotropic carbon fibers heat-treated at same temperature, it can be seen that the anisotropic carbon fibers possess larger crystal size and that these crystals grow much more markedly upon heat treatment, demonstrating the enhanced graphitizability of the anisotropic carbon fibers.

Fig. 2 shows TEM atomic lattice images of (a) IF1000, (b) IF2000, (c) IF3000, (d) AF1000, (e) AF2000 and (f) AF3000. The insets in Fig. 2(a-f) are magnified images

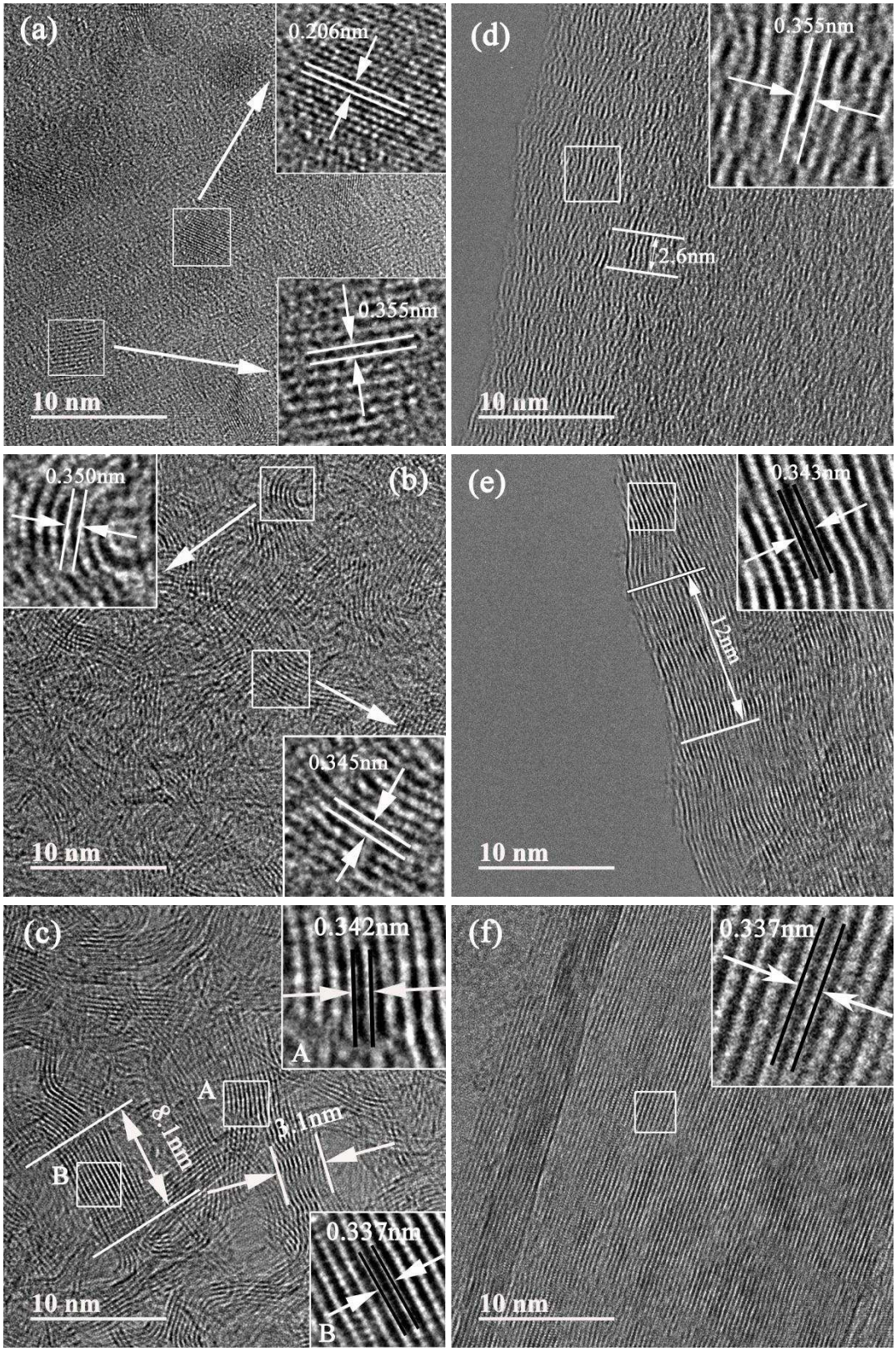

Fig. 2 Typical HRTEM images of (a) IF1000, (b) IF2000, (c) IF3000, (d) AF1000, (e) AF2000 and (f) AF3000.

of lattice fringes from the boxes marked in these figures. With increasing heat-treatment temperature from 1000 to 3000 °C, the gradual decrease in the {002} intergraphene spacing (from ca. 0.35 to ca. 0.34 nm, shown in the insets in Fig. 2(a-c)) can be readily resolved in these images, and the carbon layers of the isotropic carbon fibers become more ordered and display a less turbostratic structure. The in-plane coherence length ($La_{(100)}$) and the stack height ($Lc_{(002)}$) of the isotropic carbon fibers also increase with heat-treatment temperature, but their sizes are still only a few nanometers. This is consistent with the XRD-derived crystalline parameters of the isotropic carbon fibers shown in Table 1.

With increasing heat-treatment temperature, the mesophase pitch-based carbon fibers (shown in Fig. 2(d-f)), possess larger crystallite grains and higher orientation along the {002} plane in comparison with the isotropic carbon fibers (shown in Fig. 2a-c), even at the relatively low heat treatment temperature of 1000 °C (as shown in Fig. 2(d)). It can be seen from Fig. 2(d-f) and the insets in Fig. 2(d-f) that the d-spacing of the {002} planes of the anisotropic fibers heat-treated at 1000, 2000 and 3000 °C decreases from 0.355 to 0.343 and then 0.337 nm, whilst $La_{(002)}$ increases from 2.6 to 12 and (not shown) 66 nm, respectively. In comparison with AF1000, the graphene planes of further heat-treated AF2000 and graphitized AF3000 become progressively more ordered, suggesting that the graphitization treatment effectively promotes the crystal growth of the graphitic layers of the anisotropic carbon fibers, their layer orientation and the degree of graphitization. These results are also consistent with those of the XRD profiles in Fig. 1 and the crystalline parameters in

Table 1.

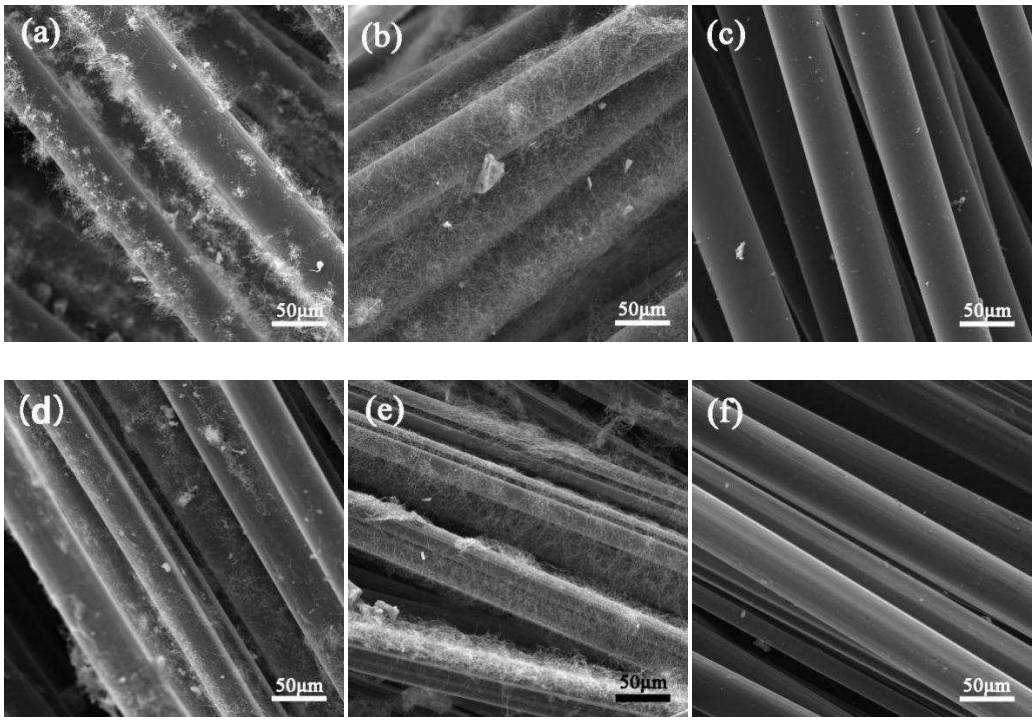

Fig. 3 SEM images of products from reaction of unpurified silicon powders with carbon fibers (a) IF1000, (b) IF2000, (c) IF3000, (d) AF1000, (e) AF2000 and (f) AF3000.

In order to understand the possible influence of the carbon sources on the formation of SiCw, the two types of carbon fibers after heat-treatment at various temperatures were used as carbon sources for reaction with silicon powders at 1400 °C. Fig. 3 shows SEM images of the products. Fig. 3(a) and Fig. 3(d) clearly show that some fibrillar materials are produced on the surface of the carbon fibers previously treated at 1000 ºC. In comparison with the former, more nanowhiskers are produced on IF2000 and particularly on AF2000 (shown in Fig. 3(b) and Fig. 3(e)). Although it is

difficult to quantify the exact yields, SEM observation of many sample regions clearly indicates that whiskers grow preferentially on the surfaces of IF2000 and AF2000. Furthermore, hardly any formation of SiCw is observed on the surface of carbon fibers treated at 3000 ºC as shown in Fig. 3(c) and Fig. 3(f), indicating that whisker formation is difficult in these cases. Disregarding the growth mechanism of SiC whiskers, if the formation of SiC nanofibers is governed by the transport and homogeneous nucleation of carbon and silicon sources on the surface of carbon fibers, it should be possible to form SiCw from any of the various carbon sources. Since this is not the case, it is likely that the significant differences in the microstructure and / or crystal size of the carbon precursors affect the formation of SiC whiskers in a heterogeneous growth process.

Fig. 4 shows TEM and HRTEM images of the product derived from reaction of Si with IF1000 at 1400 °C. Straight whiskers with diameter mainly in the range of 20-50 nm are observed in Fig. 4(a). The crystalline fringes (magnified and inset in Fig. 4(b)) have a spacing of 0.216 nm, consistent with the (200) plane spacing of cubic SiC. The SAED pattern, shown in Fig. 4(c), shows that the straight SiCw consists of single crystal SiC. The pattern can be indexed to the (111), (200) and $(1\bar{1}\bar{1})$ planes of SiC, consistent with the crystal viewed down the $[1\bar{1}1]$ axis. The relative intensities of the spots in the SAED pattern are similar to the standard XRD intensities for cubic β-SiC (ICDD database reference code: 01-073-1665).

In addition, the EDX spectrum in Fig. 4(d) shows that the nanowhisker contains Si, C and O, and the similar atomic ratio of Si and C suggests that it consists largely of

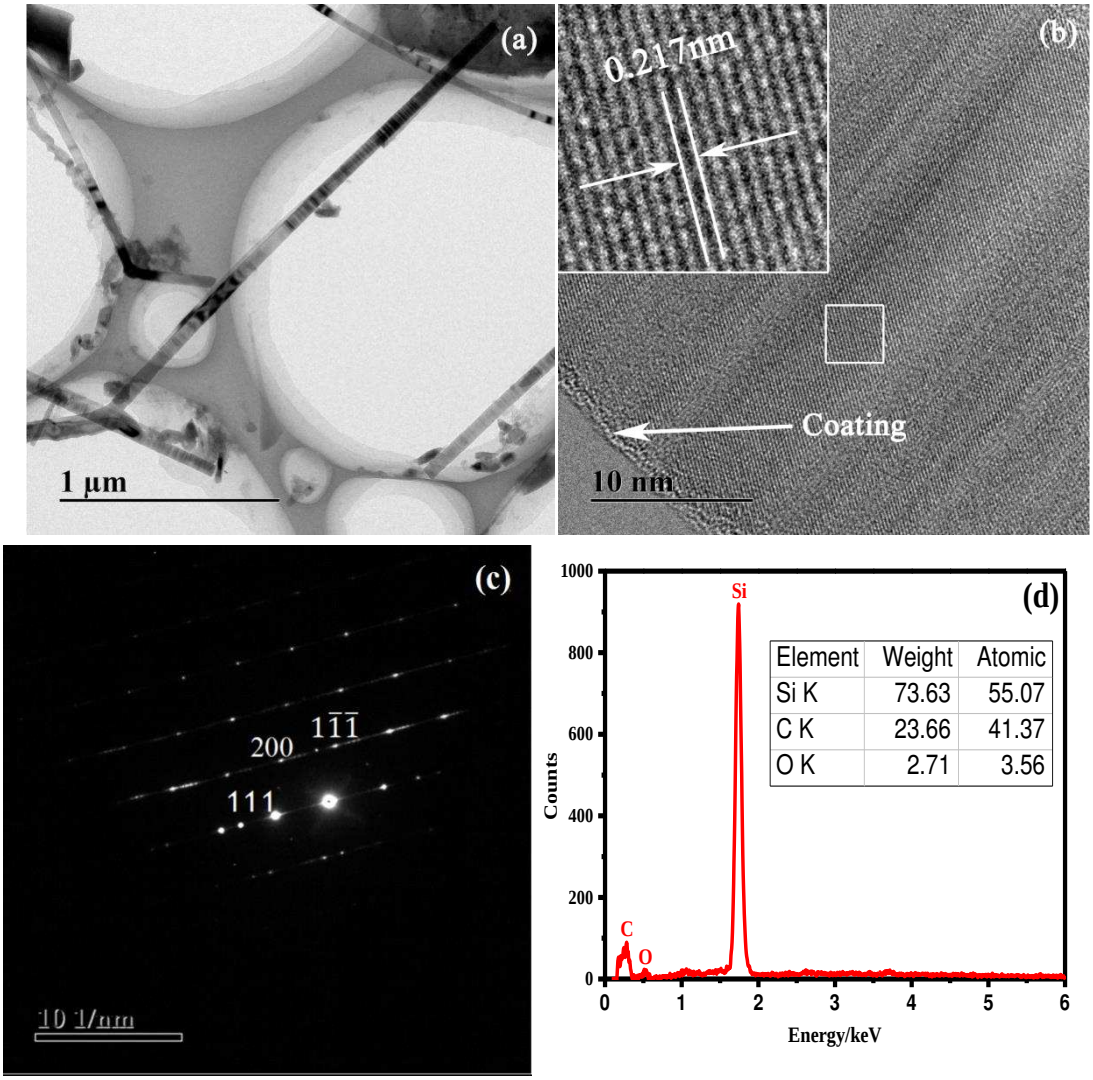

Fig. 4 (a) TEM image of products derived from the reaction of Si with IF1000 at 1400 °C; the inset in (b) is the magnified image from the box in (b) showing that the lattice fringes have a spacing consistent with the (200) plane of cubic SiC; (c) SAED pattern and (d) EDX spectrum from fibers shown in (b).

silicon carbide. The disordered edge structure of the SiC whisker in Fig. 4(b) may be attributed to SiO_2, whose existence on the surface of SiCw may imply that the formation of SiCw involves the formation of SiO which may result from the unpurified silicon powders [21]. This is because, previously, Kholmanov [21] reported

that the possible presence of infinitesimal oxygen in silicon powders could facilitate the formation of SiCw. In order to test the influence of the surface silica of silicon powders on the formation of SiCw, the as-received silicon powders were alternatively treated with hydrofluoric acid under magnetic stirring for 24 h to remove the silica component on their surfaces and, after water washing, dried at room temperature under vacuum.

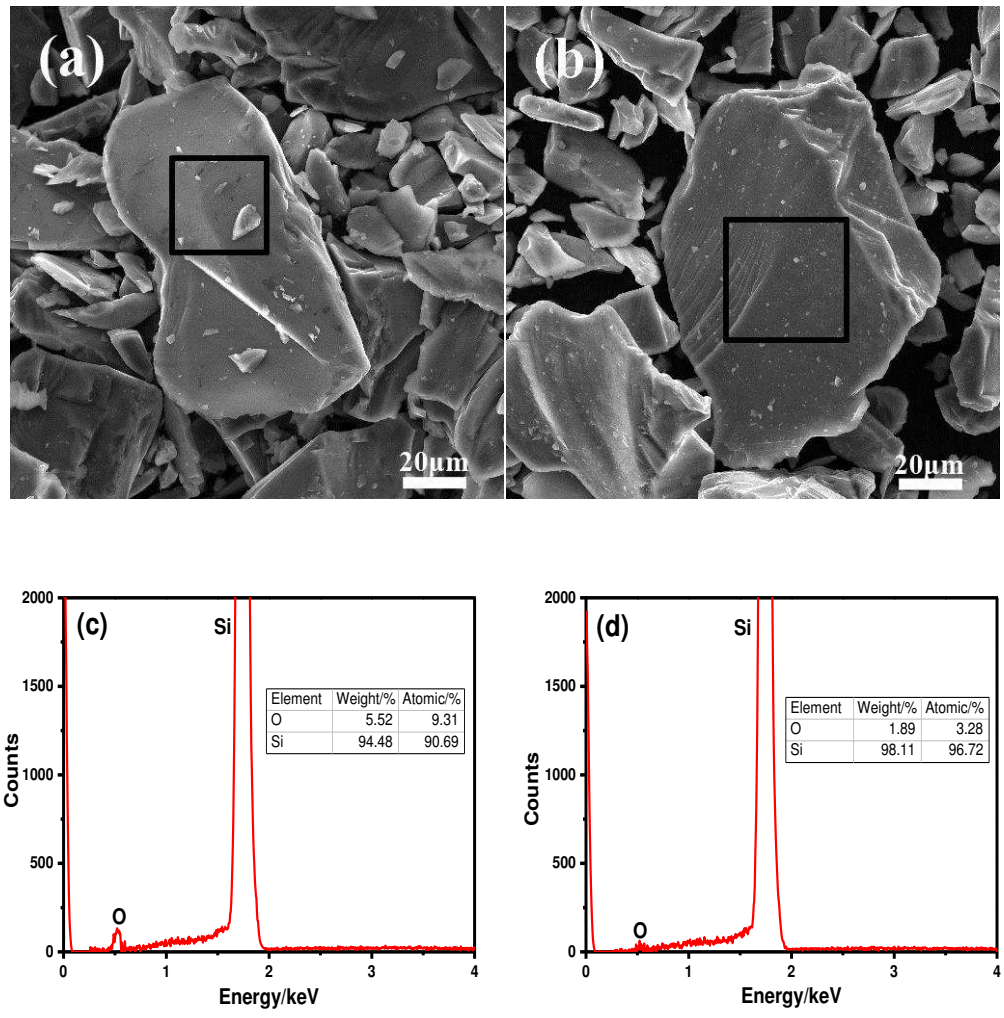

Fig. 5 SEM images of (a) silicon powders before purification, (b) silicon powders after purification, and their EDX spectra (c) and (d), respectively.

The SEM images in Fig. 5(a) and Fig. 5(b) show that the hydrofluoric acid treatment has no obvious influence on the size and morphology of the silicon powders. However, Fig. 5(c) and Fig. 5(d) show the semi-quantitative silicon and oxygen EDX elemental analyses of the as-received and HF-treated silicon powders, respectively. These indicate that the oxygen content of the silicon powders decreases from approximately 5.52 wt% to 1.89 wt% after hydrofluoric acid treatment.

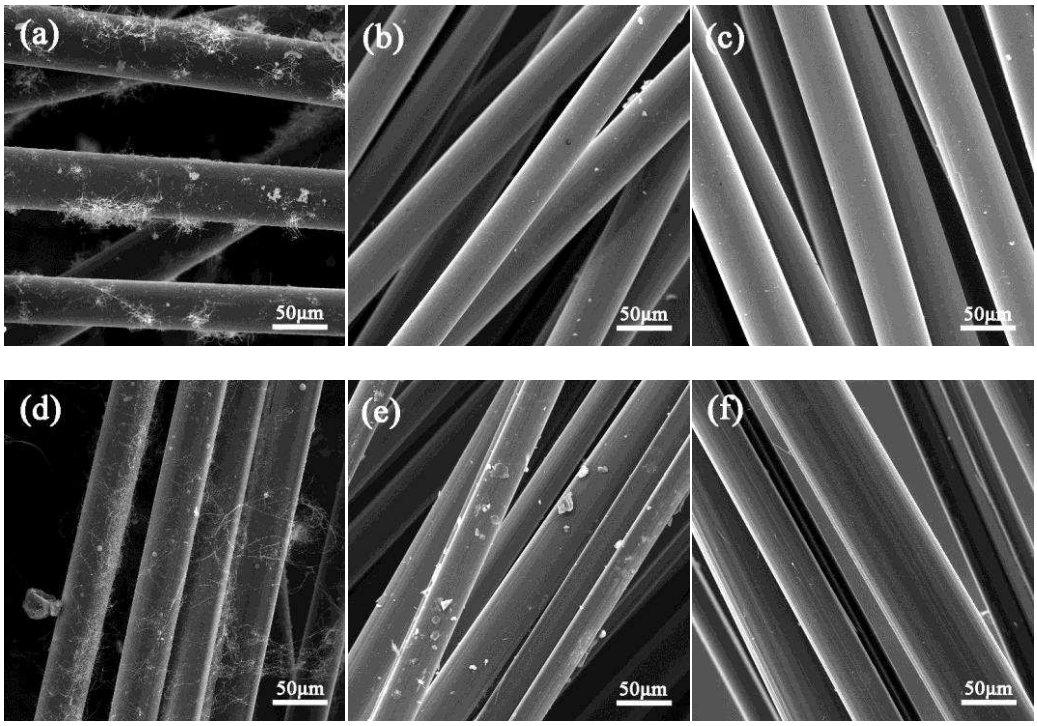

Fig. 6 SEM images of products prepared by reaction of purified silicon with (a) IF1000, (b) IF2000, (c) IF3000, (d) AF1000, (e) AF2000 and (f) AF3000 at 1400 ºC.

Fig. 6 shows SEM images of the products prepared by reaction of the six carbon fiber variants with the purified silicon powders at 1400 ºC. Compared with the products shown in Fig. 3(b) and Fig. 3(e) from reaction of unpurified silicon powders

with IF2000 and AF2000, which show a lot of SiCw formation on the fibers, no SiCw is observed on IF2000 and AF2000 (nor on IF3000 and AF3000). This suggests that SiCw cannot be formed by reaction of the carbon fibers with purified silicon due to the absence of oxygen. Only a few whiskers can been seen on the samples from IF1000 and AF1000 (shown in Fig. 6(a) and Fig. 6(d)), implying that the carbon fibers IF1000 and AF1000 contain oxygen.

Table 2 Elemental analysis of carbon fibers heat-treated at various temperatures

Carbon fibers	Elemental analysis (wt.%)		
	C	H	O
IF1000	93.74	0.77	4.94
IF2000	98.65	0.29	0.74
IF3000	99.52	Trace	Trace
AF1000	96.16	0.50	3.00
AF2000	99.55	Trace	Trace
AF3000	99.86	Trace	Trace

In order to prove the existence of oxygen in carbon fibers, elemental analysis was employed to determine the elemental content of each carbon fiber type. Table 2 illustrates the variation in relative C, H and O contents in isotropic and anisotropic pitch-based carbon fibers with respect to heat-treatment temperature. Heat-treatment at higher temperature increases the C content and reduces the H and O contents in the

carbon fibers. The carbon fibers IF1000 and AF1000 contain significant amounts of H and O, implying that this may volatilize from these two carbon fibers during their reaction with silicon. After heat treatment at 2000 ºC or graphitization at 3000 ºC, the C content in the fibers approaches 100% with little more than trace H and O content, and thus no significant scope for H or O volatilization during reaction of the fibers with silicon [27].

To further reveal the influence of these volatiles on the formation of SiC whiskers, TG–MS analysis was utilized to measure real time gas evolution during pyrolysis of the carbon fiber. This facilitates not only the quantitative assessment of the pyrolysis process but also the identification of decomposition products from the MS profiles of individual off-gases. Considering the role H_2O plays in the formation of SiO gas as shown in reaction (1) [28],

$$Si + H_2O\ (g) \rightarrow SiO + H_2 \quad (1)$$

the evolution of H_2O is of particular interest. Fig. 7 shows the evolution of H_2O in the TG–MS analyses of IF1000, IF2000 and AF1000. Since the MS signals were normalized to the mass of the sample and the maximum total intensity arising in the experiment, TG–MS allows semi-quantitative analysis. For IF1000 and IF2000, the first H_2O evolution occurs in the range of 80-300 ºC with maximum intensity at about 120 ºC and 150 ºC, respectively, corresponding to the removal of adsorbed water. In contrast, there is no obvious trace of water in AF1000 in the range of 80−300 ºC. Evolution of H_2O arises again in the pyrolyses of IF1000 and AF1000 above 300 ºC with an increasing release rate over the course of the experiment. In contrast, there is

no evident H_2O evolution during the pyrolysis of IF2000, in accordance with its low H and O content, as shown by elemental analysis. This suggests that carbon fiber pyrolyzed at a lower temperature (1000 °C) may still release some H_2O vapor during later reaction with silicon, leading to the growth of SiC whiskers via to the formation of SiO, in agreement with the results shown in Fig. 6(a) and Fig. 6(d). The suggested

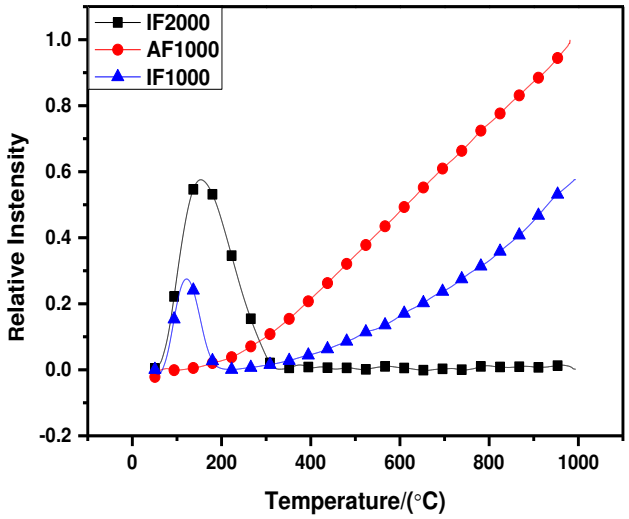

Fig. 7 TG-MS analysis of evolution of H_2O in AF1000, IF1000 and IF2000.

formation and growth mechanism of SiC whiskers is as follows:

$$Si + H_2O\ (g) \rightarrow SiO + H_2 \qquad (1)$$

$$SiO + 2C \rightarrow SiC + CO \qquad (2)$$

$$SiO + 3CO \rightarrow SiC + 2CO_2 \qquad (3)$$

$$C + CO_2 \rightarrow CO \qquad (4)$$

Once gaseous silicon monoxide (SiO) was formed following reaction (1), the gaseous SiO product subsequently reacts with C and CO according to reactions (2) and (3),

respectively. As a result, silicon carbide will be produced by heterogeneous nucleation according to reaction (2) [14,23]. In addition, further growth of SiC whiskers is believed to occur via the gas-phase process in reaction (3). Once CO_2 is produced in reaction (3), this further reacts rapidly and spontaneously with nearby carbon fibers to form CO gas continuously according to reaction (4), thereby continuing the abovementioned cycle.

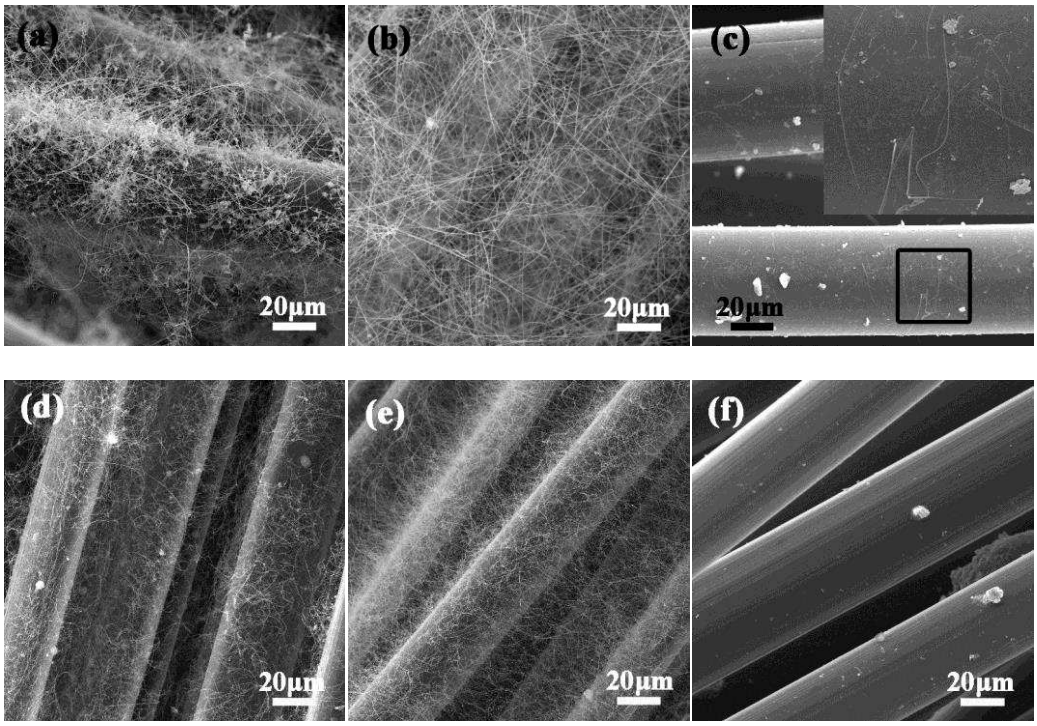

Fig. 8 SEM images of products from reaction of silica and silicon mixture with (a) IF1000, (b) IF2000, (c) IF3000, (d) AF1000, (e) AF2000 and (f) AF3000 at 1400 °C.

To further study the influence of gaseous SiO on the formation of SiC whiskers, the reactivity of carbon fibers with a mixture of silicon and silica was investigated and the SEM images of products as-prepared at 1400 °C are shown in Fig. 8. Silica powders

were introduced to maintain an abundance of SiO in the atmosphere, derived from the reaction of silicon with silica. Compared with the products shown in Fig. 3(a and b) and Fig. 3(d and e), the yield of SiC whiskers shown in Fig. 8(a and b) and Fig. 8(d and e) is markedly increased. This demonstrates that abundant SiO gas is beneficial to the formation and growth of SiC whiskers. Furthermore，SiC whiskers still grow preferentially on the surface of carbon fibers treated at 2000 °C and cannot be seen on the surface of AF3000. A few whiskers can be observed from IF3000 as shown inset in Fig. 8(c). Even after taking account of the influence of silicon source, different growth SiCw behaviors are still exhibited on the surfaces of the differing carbon fibers. This may be attributed to heteroepitaxial growth of SiC on carbon fibers with various microstructures.

With respect to heteroepitaxial nucleation and growth, a great deal of work has been reported, which demonstrates that heteroepitaxial growth is energetically favorable due to the relatively small lattice mismatch between substrates and heteroepitaxial growth products [29,30]. The relatively close correspondence between the graphite 100 d-spacing (0.213 nm) and the cubic SiC 200 d-spacing (0.217 nm) might at first sight suggest that single crystal SiCw growth may occur epitaxially on the carbon fibers with little strain in an energetically favourable manner, (although this would not explain why no significant SiC growth occurs on IF3000 or AF3000). To explore the above conjecture, the d-spacings giving rise to the {100} diffraction peak for carbon fibers heat treated at various temperatures will be considered. Fig. 9 shows these {100} diffraction peaks from the carbon fibers treated at various temperatures. The XRD

patterns from carbon fibers treated at up to 2000 °C show broad {100} diffraction peaks, suggesting that a significant proportion of their 100 d-spacings may be greater than 0.213 nm, the 100 d-spacing of perfect graphite, and near to 0.217 nm, the 200 d-spacing of cubic SiC. Therefore, SiC whiskers as shown in Fig. 8(a and b) and Fig. 8(d and e) are easy to nucleate and grow on some areas of the carbon fibers treated at up to 2000 °C. On the other hand, the graphite 100 d-spacings of carbon fiber AF3000 are tightly clustered around 0.213 nm, i.e. significantly less than the 0.217 nm 200 d-spacing of cubic SiC, meaning that epitaxial growth of SiC on this carbon is not favoured. The larger crystal size of carbon fiber AF3000 (shown in Fig. 2(f) and Table 1) also tends to disfavor growth of SiCw.

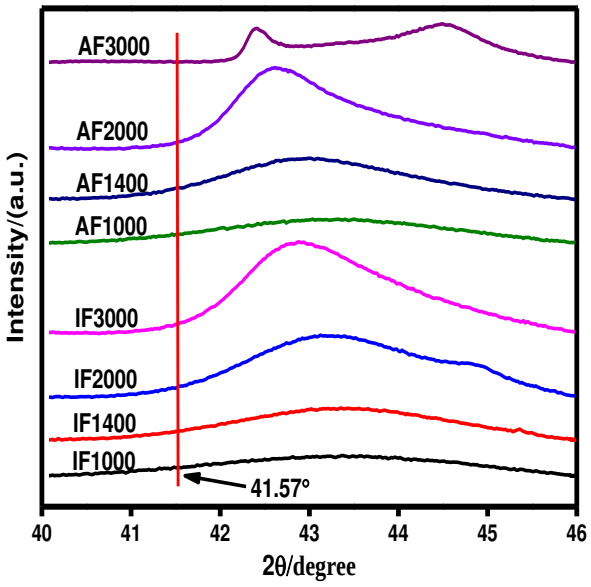

Fig. 9 XRD patterns in the region of the {100} diffraction peak of carbon fibers heat-treated at various temperatures. 2θ=41.57° corresponds to 0.217 nm, i.e. the 200 d-spacing of cubic SiC.

As shown in Fig. 2(c), the carbon fiber IF3000 is composed of both straight and curved carbon layer crystal grains. The areas composed of straight carbon layers have a lower d_{002} value (0.337 nm) and a d_{100} value near to 0.213 nm, similar to those of carbon fiber AF3000, so epitaxial growth of SiCw is not favoured on this carbon structure. The areas composed of curved carbon layers may have larger more epitaxially compatible d_{100} values; however, geometrical consideration of this curved structure suggests that its $La_{(100)}$ is quite low, meaning that areas suitable for epitaxial growth are limited in size and hence few SiC whiskers are formed on IF3000 carbon fiber. This analysis suggests that carbon fibers must contain tubostratically stacked graphite structure and possess an appropriate grain size to favour significant formation of SiC whiskers.

In order to understand the possible influence of the reactivity of graphite fibers with defective carbon structure on the formation and growth of SiCw, the graphite fiber AF3000 was oxidized at 600 °C under air for 3 h or in a mixture of sulfuric acid (98 wt%) and nitric acid (65 wt%) with volume ratio of 7:3 for 48 h. The acid oxidized sample was finally washed in distilled water to neutrality and dried at 100 °C for 24 h. Fig. 10 shows the Raman spectra and SEM images of the surfaces of AF3000 and its air- and acid-oxidized derivatives. In comparison with AF3000, the intensity of G peak at 1585 cm^{-1} (shown in Fig. 10(a)) of the two samples after air and acid oxidations do not show obvious change, indicating the air or acid oxidations have little influence on the crystal structure of graphite fibers. However, the intensity of the D peak of the two samples after air and acid oxidation became stronger compared

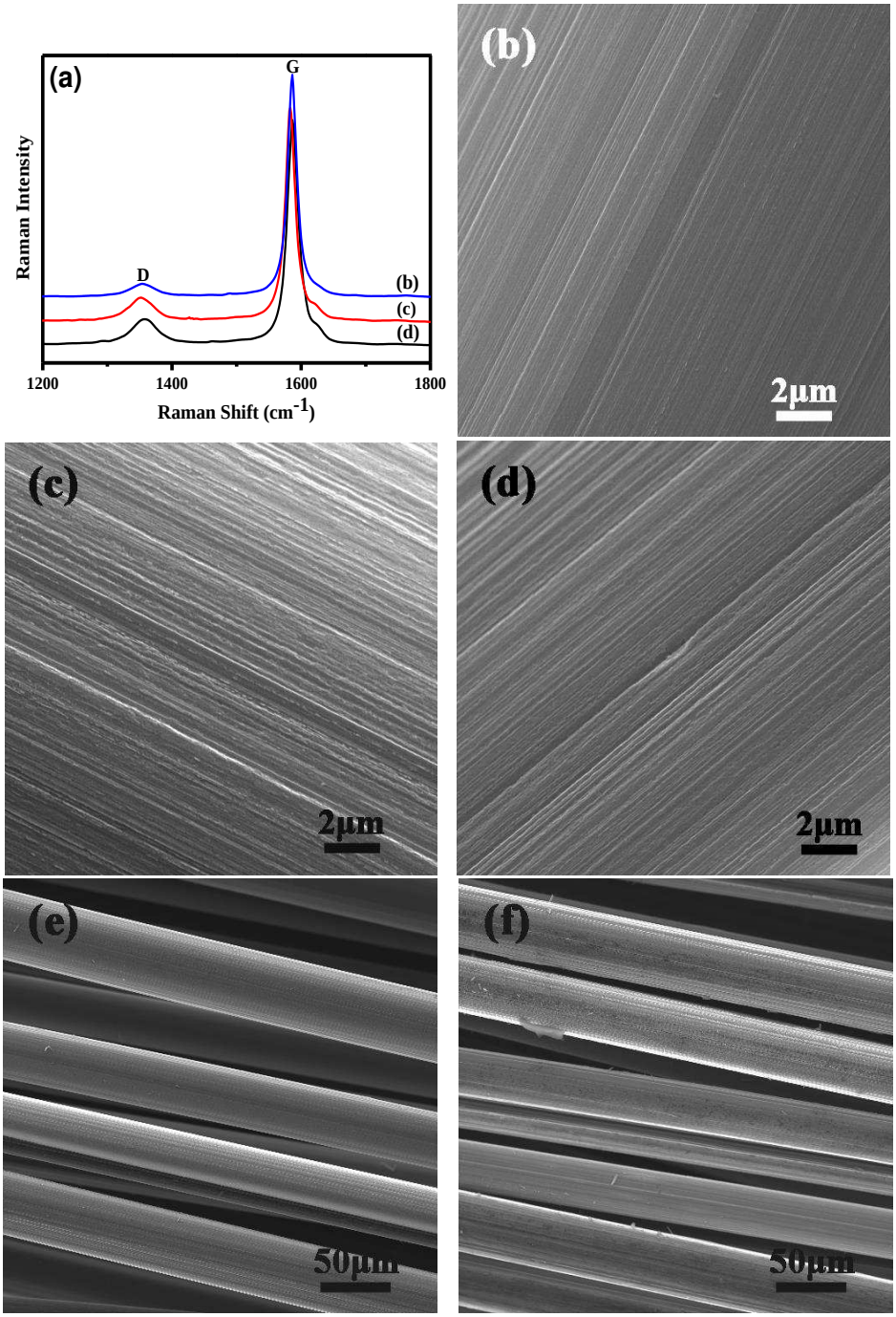

Fig. 10 Raman spectra (a) and SEM images of (b) AF3000, (c) AF3000 oxidized in air and (d) AF3000 oxidized in acid; the corresponding SEM images of products from reaction of the mixture of silica and silicon with AF3000 oxidized in the air and AF3000 oxidized in acid at 1400 °C for 1 h are shown in Fig. 10(e and f).

with that of the original AF3000, showing that air and acid oxidations lead to the

formation of defects on the surface of the two samples. In comparison with sample AF3000, rough surfaces can be observed upon oxidation of graphite fibers, which is in good agreement with the results of Raman spectra.

The two oxidized graphite fibers were used as carbon source for the synthesis of SiC whiskers by reacting them with a mixture of silica and silicon at 1400 °C for 1 h. No SiC whiskers can be seen in the SEM images of the products (Fig. 10(e and f)). Thus the existence of defects on the surface of graphite fiber seems to have not direct relation with the growth of SiC whiskers. The effect of deeper oxidation treatment on the crystal structure of graphite fibers and the growth of SiC whiskers thereon will be investigated in our future work.

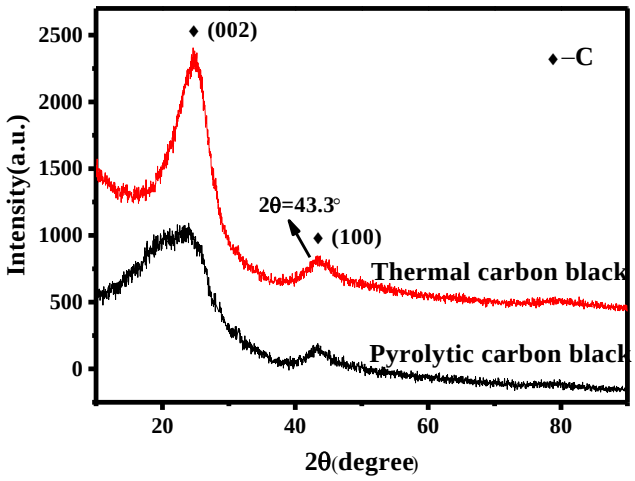

Fig. 11 XRD patterns of pyrolytic carbon black and thermal carbon black.

The effect of carbon materials microstructure on the formation and growth of SiC whiskers was also investigated by reaction of nanosized pyrolytic carbon black and microsized thermal carbon black with a mixture of silica and silicon at 1400 °C for 1

h. The XRD patterns of pyrolytic carbon black and thermal carbon black, shown in Fig. 11, show two weak and broad peaks at about 2θ = 25 and 43.3°, corresponding to the {002} and {100} / {101} planes of graphitic carbon, respectively. Their breadth and the absence of other peaks indicate that both are mainly composed of a rather amorphous carbon structure.

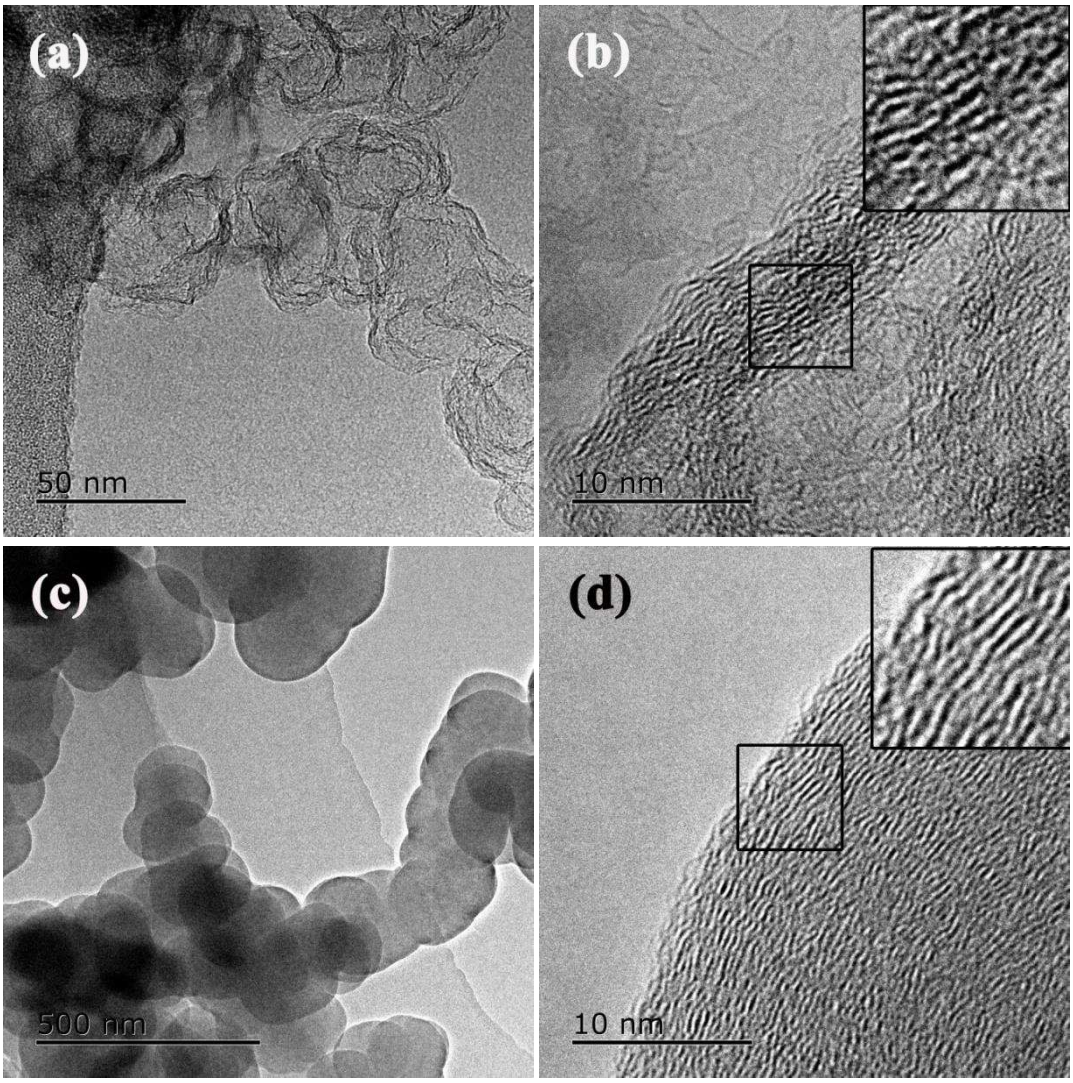

Fig. 12 Typical TEM and HRTEM images of (a,b) pyrolytic carbon black and (c,d) thermal carbon black.

Fig. 12 shows typical TEM and HRTEM images of (a,b) pyrolytic carbon black and (c,d) thermal carbon black. The TEM images show that the pyrolytic carbon black and thermal carbon black consist of agglomerated particles that are spherical and possess the diameters in the range of 20-50 and 120-500 nm, respectively (Fig. 12(a and c)). However, the pyrolytic carbon black and thermal carbon black shown in Fig. 12(a) and Fig. 12(c) display hollow ball and solid spherical particle morphologies, respectively. Fig. 12(b and d) show the TEM atomic lattice images of pyrolytic carbon black and thermal carbon black. They show that the two carbon sources are composed of turbostratic graphitic structure, which is consistent with the results of XRD in Fig. 11. The insets in Fig. 12(b and d) are the magnified images of the lattice fringes from within the corresponding marked boxes in Fig. 12(b and d). The intergraphene spacing of ca. 0.35 nm for the {002} plane of graphitic carbon can be readily resolved in these images. It seems that the pyrolytic carbon black shown in Fig. 12(a and b) is composed of ribbon-shaped carbon layers and forms an enclosed hollow ball. The thermal carbon black shown in Fig. 12(d) is composed of curved carbon layers and displays an onion-like structure. No obvious differences are observed between the edge structure of the nanosized pyrolytic carbon black and microsized thermal carbon black shown in Fig. 12(b and d), respectively. In comparison with the edges of two carbon blacks, the centers of nanosized pyrolytic carbon black and microsized thermal carbon black display a hollow structure and a more turbostratic structure, respectively.

After reaction of the mixture of silica and silicon with pyrolytic carbon black and thermal carbon black at 1400 °C, the SEM images of the products are shown in Fig.

13(a and b), respectively. A lot of SiC whiskers are clearly observed in the product prepared from pyrolytic carbon black (Fig. 13(a)). In contrast, few SiC whiskers can be found in the product prepared from thermal carbon black (Fig. 13(b)). This implies that the latter's curved carbon layers are disadvantageous for the nucleation and growth of SiC whiskers, perhaps because a curved carbon substrate disfavours

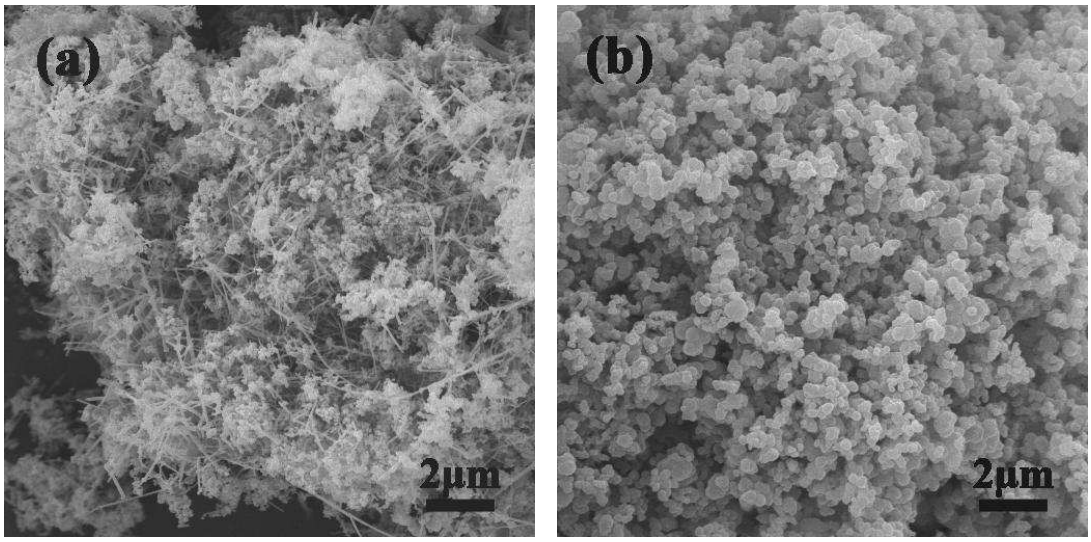

Fig. 13 SEM images of products derived from reaction of silica and silicon mixture with (a) pyrolytic carbon black and (b) thermal carbon black at 1400 °C for 1 h.

epitaxial growth. In our ref. [29], we said that single crystal TiC was formed more readily on pyrolytic carbon black and MWCNTs rather than on thermal black and lamp black, because thermal (and even lamp) carbon black seem to have a higher $La_{(100)}$ than pyrolytic carbon black. Ref. [29] explained that single crystal TiC growth was limited by large carbon stack heights (> 15 nm) as these were expected to lead to a breakdown in interfacial coherency due to a build-up of interfacial strain when slight epitaxial mismatches are amplified over longer distances. In the present

manuscript, the invocation of curvature as an impediment to epitaxial growth is therefore an alternative explanation as to why carbide formation may be hindered. It indicates that the defective structure of the carbon source is not a unique critical factor for the growth of SiC whiskers. Instead, the curvature of the carbon layers as well as the grain size and the d-spacing of {002} and {100} planes of carbon sources may have a more significant influence on the growth of SiC whiskers.

4. Conclusions

SiC whiskers were synthesized successfully at 1400 °C by the reactions of mixed silicon and silica powders with isotropic or anisotropic carbon fibers previously treated at 1000 and 2000 °C as carbon sources. The resulting SiC whiskers are mainly composed of single crystal nanofibers and have diameters mostly in the range 20–50 nm. The formation of some SiC whiskers was also observed by reaction of (particularly isotropic) carbon fiber treated at 1000 °C with purified, oxygen-free, silicon powders, which can be attributed to the formation of SiO by reaction of Si with water released from the carbon fibers. The presence of SiO as silicon source is a precondition for the formation and growth of SiC whiskers. It was also demonstrated that SiC whisker growth is favoured on the surface of carbon fibers with suitable d_{100} and $La_{(100)}$ values by an epitaxial growth mechanism. Carbon fibers must therefore contain tubostratic stacking graphite structure and possess an appropriate grain size to facilitate formation of SiC whiskers. Supplementary studies, using air- or acid-oxidized AF3000 fibers show that introduction of defects on the surface of the graphite fibers does not encourage growth of SiC whiskers. In addition, defective

carbon sources, such as thermal carbon black and pyrolytic carbon black, were used to grow SiC whiskers. These results also indicate that defective carbon structure is not the unique critical factor for the growth of SiC whiskers. The understanding gained through this study therefore offers possibilities for large scale preparation of SiC whiskers using carbon sources with defined structure by a carbothermal reduction synthesis method. In future studies, following further elucidation of the nucleation and growth mechanisms of the carbides, control of the carbide product yield is expected to be achievable by tailored variation of the synthesis conditions.

Acknowledgements

This work was sponsored by the Key Program of the Major Research Plan of the National Natural Science Foundation (Grant No. 91016003) and the National Natural Science Foundation (Grant No. 51372177) of China.

References

[1] Wong EW, Sheehan PE, Lieber CM. Pyrolyticbeam mechanics: elasticity, strength, and toughness of pyrolyticrods and pyrolytictubes. Science 1997;277(5334):1971−5.

[2] Fan JY, Wu XL, Chu PK. Low-dimensional SiC pyrolyticstructures: Fabrication, luminescence, and electrical properties. Prog Mater Sci 2006;51(8): 983−1031.

[3] Horaguchi I, Afaghani JED, Yamaguchi K, Nakamoto T. Characterization and application of the sliding wear of hardened die steel against SiC whisker-plastic composite. Wear 1996;198(1−2):229−35.

[4] Afaghani JED, Yamaguchi K, Horaguchi I, Nakamoto T. Whisker behaviors and tool wear in cutting of unidirectional SiC whisker-reinforced plastic. Wear 1996;195 (1−2):223−31.

[5] Li HJ, Fu QG, Shi XH, Li KZ, Hu ZB. SiC whisker-toughened SiC oxidation protective coating for carbon/carbon composites. Carbon 2006;44(3):602−5.

[6] Musa C, Orrù RS, Diletta S, Laura C, Cao G. Synthesis, consolidation and characterization of monolithic and SiC whiskers reinforced HfB_2 ceramics. J Eur Ceram Soc 2013;33(3):603−14.

[7] Lee DY, Yoon DH. Properties of alumina matrix composites reinforced with SiC whisker and carbon pyrolytictubes. Ceram Int 2014;40(9):14375−83.

[8] Pozuelo M, Kao WH, Yang JM. High-resolution TEM characterization of SiC pyrolyticwires as reinforcements in a pyrolyticcrystalline Mg-matrix. Mater Charact 2013;77:81−8.

[9] Park JH, Kim WJ, Kim DJ, Ryu WS, Par JY. Selective growth of β-SiC whisker on a patterned Si (111) substrate for a field emission device. Thin Solid Films 2007;515(13):5519−23.

[10] Chen JJ, Zhang JD, Wang MM, Li Y. High-temperature hydrogen sensor based on platinum pyrolyticparticle-decorated SiC pyrolyticwire device. Sens Actuators B Chem 2014;201:402−6.

[11] Li F, Wen G, Song L. Growth of pyrolyticwires from annealing SiBONC pyrolyticpowders. J Cryst Growth 2006;290(2):466−72.

[12] Tang CC, Fan SS, Dang HY, Zhao JH, Zhang C, Li P, Gu Q. Growth of SiC

pyrolyticrods prepared by carbon pyrolytictubes-confined reaction. J Cryst Growth 2000;210 (4):595−9.

[13] Fu QG, Li HJ, Shi XH, Li KZ, Hu ZB, Wei J. Microstructure and growth mechanism of SiC whiskers on carbon/carbon composites prepared by CVD. Mater Lett 2005;59(19-20):2593−7.

[14] Li XK , Liu L. Zhang YX, Shen SD , Ge S, Ling LC. Synthesis of pyrolyticmetre silicon carbide whiskers from binary carbonaceous silica aerogels. Carbon 2001;39 (2):159−65.

[15] Li B, Song YC, Zhang CR, Yu JS. Synthesis and characterization of pyrolyticstructured silicon carbide crystal whiskers by sol-gel process and carbothermal reduction. Ceram Int 2014;40(8):12613−6.

[16] Li J, Shirai T, Fuji M. Rapid carbothermal synthesis of pyrolyticstructured silicon carbide particles and whiskers from rice husk by microwave heating method. Adv Powder Technol 2013;24(5):838−43.

[17] Cetinkaya S, Eroglu S. Chemical vapor deposition of C on SiO_2 and subsequent carbothermal reduction for the synthesis of pyrolyticcrystalline SiC particles/whiskers. Int J Refract Met Hard Mater 2011;29(5):566−72.

[18] Wei J, Li KZ, L HJ, Ouyang HB, Li ZJ, Wang C. Photoluminescence performance of SiC pyrolyticwires, whiskers and agglomerated pyrolyticparticles synthesized from activated carbon. Physica E 2009;41(8):1616−20.

[19] Ryu Z, Zheng JT, Wang MZ, Zhang BJ. Synthesis and characterization of silicon carbide whiskers. Carbon 2001;39(12):1929−30.

[20] Satapathy LN, Ramesh PD, Agrawal D, Roy R. Microwave synthesis of phase-pure, fine silicon carbide powder. Mater Res Bull 2005;40(10):1871−82.

[21] Kholmanov IN, Kharlamov A, Barborini E, Lenardi C, Li Bassi A. Bottani CE, et al. A simple method for the synthesis of silicon carbide pyrolyticrods. J Pyrolyticsci Pyrolytictech 2002;2(5):453−6.

[22] Zhou D, Seraphin S. Production of silicon carbide whiskers from carbon pyrolyticclusters. Chem Phys Lett 1994;222(3):233−8.

[23] Wu YJ, Qin W, Yang ZX, Wu JS, Zhang YF. Preparation of high-quality β-SiC pyrolyticwhiskers by using carbon fibres as carbon source. J Mater Sci 2004;39:5563−5.

[24] Wu YJ, Qin W, Yang ZX, Wu JS, Zhang YF. Synthesis of β-SiC pyrolyticwhiskers by high temperature evaporation of solid reactants. Mater Lett 2004;58(17):2295-8.

[25] Iwashuta N, Park CR, Fujimoto H, Shiraishi M, Inagaki M. Specification for a standard procedure of X-ray diffraction measurement on carbon materials. Carbon 2004;42(4):701−14.

[26] Xu ZW, Liu LS, Huang YD, Sun Y, Wu XQ, Li JL. Graphitization of polyacrylonitrile carbon fibers and graphite irradiated by γ rays. Mater Lett 2009;63(21):1814−6.

[27] Korai Y, Hong SH, Mochida I. Development of longitudinal mesoscopic textures in mesophase pitch-based carbon fibers through heat treatment. Carbon 1999;37(2):203−11.

[28] Koh YH, Kwon OS, Hong SH, Kim HE, Lee SK. Improvement in oxidation resistance of carbon by formation of a protective SiO_2 layer on the surface. J Eur Ceram Soc 2001;21(13):2407−12.

[29] Li XK, Dong ZJ, Westwood A, Brown A, Brydson R, Walton A, et al. Low-temperature preparation of single crystal titanium carbide pyrolyticfibers in molten salts. Cryst Growth Des 2011;11(7):3122−9.

[30] Tu CH, Chen W, Fang HC, Tzeng Y, Liu CP. Heteroepitaxial nucleation and growth of graphene pyrolyticwalls on silicon. Carbon 2013;54:234−40.